Plastic Deformation Analysis in Parallel Tubular Channel Angular Pressing (PTCAP)

GH. Faraji[a,*], M. Mousavi Mashhadi[a]

[a] *Department of Mechanical Engineering, University of Tehran, Tehran, Iran.*

ARTICLE INFO

Article history:

Received 17 Nov 2013
Accepted 10 Dec 2013
Available online 25 Dec. 2013

Keywords:

Parallel tubular channel angular pressing
processes parameters
Finite element method
Plastic deformation

ABSTRACT

Parallel tubular channel angular pressing (PTCAP) process is a novel recently developed technique of severe plastic deformation for fabrication of ultrafine grained (UFG) metallic tubes. This new process consists of two half cycles and is affected by several parameters such as channel angles, deformation ratio and curvature angles. In this paper, the effects of these parameters on plastic deformation behavior, imposed strain, strain homogeneity and the process load were investigated by using finite element method (FEM). The results indicated that an increase in the channel angle leads to a decrease in the imposed strain at the end of both half cycles of PTCAP process. Investigation on the effects of the curvature angles showed that better strain homogeneity is achieved in lower curvature angles. Also, minimum required process load and the best strain homogeneity could be obtained in the curvature angle equal to zero. Study on deformation ratio (K) revealed that the best and worse strain homogeneity could be achieved in K values equal to 0.6 and 1, respectively. With regard to better strain homogeneity and needing lower process loads, it could be concluded that lower K value (0.6 t_0) leads to best strain homogeneity and lowest process load.

1. Introduction

Excellent mechanical properties of ultra fine grained (UFG) and nanograined (NG) materials attracted many researchers during this two past decades [1]. Severe plastic deformation (SPD) techniques are considered as a powerful tool for production of ultra-fine-grained (UFG) metals with enhanced mechanical properties [2]. The common SPD techniques suitable for bulk and sheet materials are equal channel angular pressing (ECAP) [3], high pressure torsion (HPT) [4], accumulative roll bonding (ARB) [5], accumulative torsion back processing [6], repetitive forging using inclined punch [7], and other SPD methods. Despite the demands for high strength metallic tubes in extensive range of industrial applications, few researches have been carried out for producing UFG tubular parts using SPD methods. It is may be due to lack of an appropriate SPD method suitable for deforming tubes. Through understanding the beneficial capabilities of the ECAP, an

Corresponding author:
E-mail address: ghfaraji@ut.ac.ir (GHader Faraji).

effective process suitable for processing tubes to very high strains, called the tubular channel angular pressing (TCAP) method, was proposed for the first time by the present authors [8-10]. Faraji et al. [8, 9] proposed TCAP process using triangular and semicircular channels which was previously investigated using FEM experiments. TCAP process could be influenced by several parameters. Faraji et al. [11] investigated the effects of curvature angle, deformation ration and deformation direction on plastic deformation behavior using FEM. Recently, they proposed another effective SPD method entitled PTCAP [12] which has two important advantages compared to the previously developed TCAP process. Needing lower loads and introducing better strain homogeneity through the tube thickness are two advantages [13].

As shown in Fig. 1, in the PTCAP process the constrained tube between mandrel and die is pressed by a first hollow cylindrical punch into a tubular angular channel so that the tube diameter increases to reach its maximum value at first half cycle (Fig. 1(a). In the second half cycle of PTCAP process as shown in Fig. 1(b), the tube is pressed back to its initial dimension through the tubular angular channel by the second punch. Die parameters are shown in Fig. 1(d). As can be seen in this figure, there are two shearing zones (I and II) which are acting in both half cycles.

During the first and second half cycles of PTCAP, tensile and compression peripheral strains are applied respectively. The following equation [11] can be used in conventional ECAP:

$$\bar{\varepsilon} = \left[\frac{2\cot(\phi/2 + \psi/2) + \psi \operatorname{cosec}(\phi/2 + \psi/2)}{\sqrt{3}} \right] \quad [1]$$

Considering the existence of radial and circumferential strains in PTCAP [12], the exact value of total accumulated strain $\bar{\varepsilon}_T$ in the first half cycle of PTCAP processing can be calculated by the following equation, considering the geometry of Fig. 1(c) [12]:

$$\bar{\varepsilon}_T = \sum_{i=1}^{2} \left[\frac{2\cot(\varphi_i/2 + \psi_i/2)}{\sqrt{3}} + \frac{\psi_i \operatorname{cosec}(\varphi_i/2 + \psi_i/2)}{\sqrt{3}} \right] + \frac{2}{\sqrt{3}} 1 \quad [2]$$

where R_2 and R_1 are shown in Fig. 1(d). Finally, total equivalent strain after N passes of PTCAP can be expressed in a general form by the following equation:

$$\bar{\varepsilon}_{TN} = 2N \left\{ \sum_{i=1}^{2} \left[\frac{2\cot(\varphi_i/2 + \psi_i/2)}{\sqrt{3}} + \frac{\psi_i \operatorname{cosec}(\varphi_i/2 + \psi_i/2)}{\sqrt{3}} \right] + \frac{2}{\sqrt{3}} \ln \frac{R_2}{R_1} \right\} \quad [3]$$

There are several parameters such as channel angles, deformation ratio and curvature angles in PTCAP process which affect deformation behavior and the required load. In this paper, the effects of these parameters on plastic deformation behavior, imposed strain, strain homogeneity and required load were investigated by using finite element method (FEM) for the first time.

2. Experimental

A commercial FE code Abaqus/Explicit was used to perform the numerical analysis. An axisymmetric four node elements (CAX4R) was employed to model the tube. The die and punches were modeled as analytical rigid parts. During simulations adaptive meshing was used to accommodate the large strains [7]. The Coulomb friction and penalty method were used to consider the contact between the die and the tube and the friction coefficient was assumed to be 0.05 [14, 15]. The material used for the tube sample is commercially pure copper. The experimental alloy properties, process parameters and their values are shown in Table 1. Mechanical properties of pure copper were obtained through a compression test at room temperature and strain rate of $1x10^{-5}$ sec^{-1}.

3. Results and Discussion

3. 1. Effects of channel angle $\varphi_1 = \varphi_2$

Fig. 2 shows the effects of channel angle $\varphi_1 = \varphi_2$ on plastic strain contour after the first and the second half cycle of the PTCAP process. It can be seen that increase in the

Table 1. Pure copper properties and process parameters.

Parameter	Value
Density (ρ)	8.1 g/cm3
Poisson's ration (ν)	0.33
Young's modulus (E)	120 GPa
Friction coefficient (μ)	0.05
Channel angle ($\varphi_1 = \varphi_2$)	100°, 110°, 120°, 135°, 150°, 160°
Curvature angle ($\psi_1 = \psi_2$)	0°, 10°, 20°, 30°
$K = R_2 - R_1$	0.6 t_0, 0.8 t_0, 1 t_0, 1.2 t_0, 1.4 t_0
Tube outer diameter	20 mm
Tube thickness (t_0)	2.5 mm

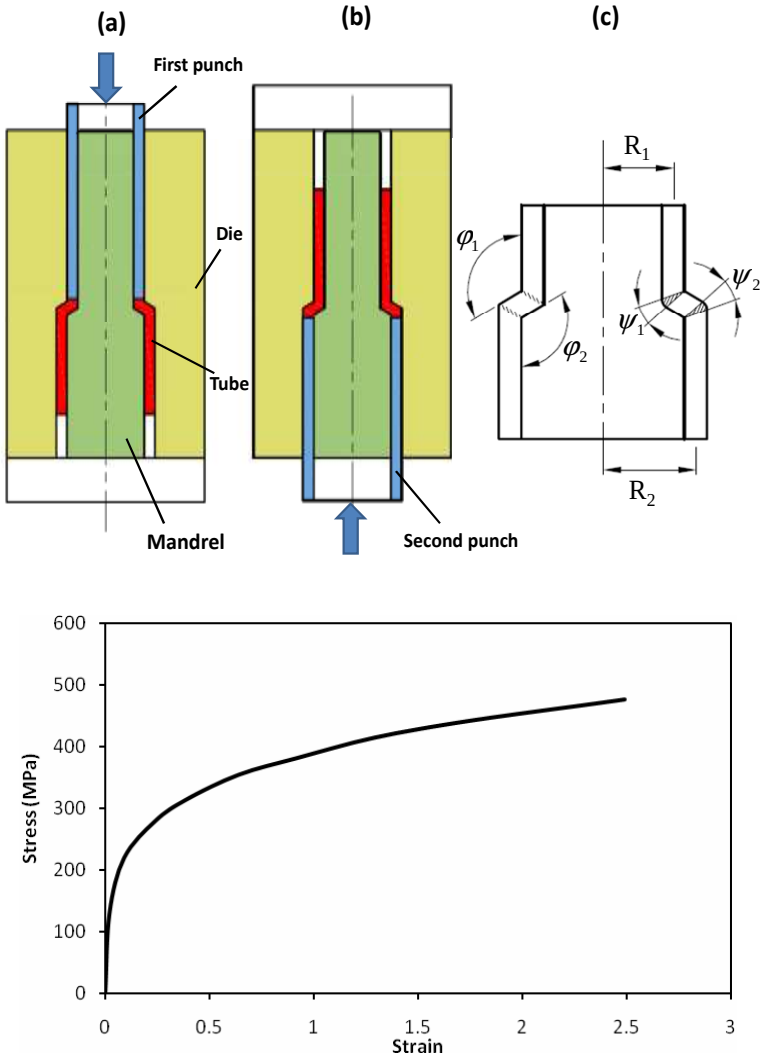

Fig. 1. Schematic of the PTCAP process (a) the first and (b) the second half cycles of PTCAP, (c) die parameters, (d) stress-strain curve of pure copper.

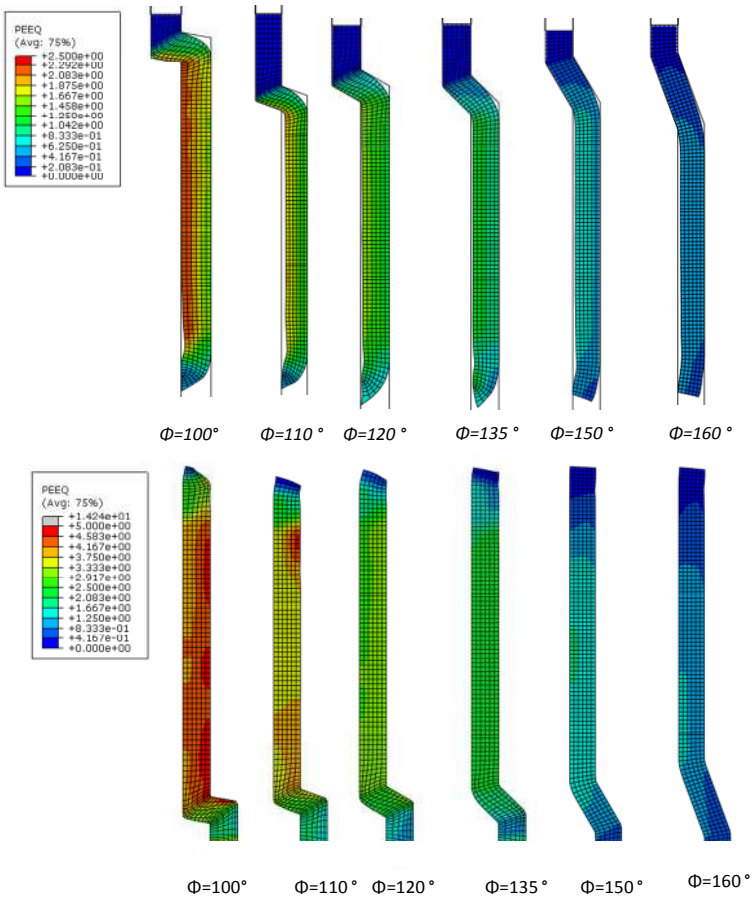

Fig. 2. Effects of the channel angle on plastic strain contour of PTCAP processed sample after (a) the first half cycle, (b) the second half cycle (in all cases; $\psi_1 = \psi_2 = 0$, $K=1$)

channel angle leads to decrease in the imposed strain at the end of both half cycles. At the end of the first half cycle some tube thinning takes place and the tube thickness is lower than its initial value due to the peripheral tensile strains. Tensile peripheral strain is applied as a result of increasing in the tube diameter [8]. As shown in Fig. 2(a), minimum tube thinning is taking place in the channel angle 100°. It may be due to the existence of higher hydrostatic pressure effect in this case compared to the other cases. This phenomenon also takes place in multi pass ECAP process [16, 17]. Existence of hydrostatic pressure in the first corner resulted from next corners leads to compensation for some tube thinning. Tube thinning reaches its minimum and maximum levels in the channel angles of 110° and 100°, respectively. Considering the tail part of the processed tube after the first half cycle in Fig. 2(a), it is clear that increase in the channel angle causes the decrease in the wasted useless part of the tube. However, tube thinning is compensated in the second half cycle due to the imposition of compression peripheral strains as a result of the decrease in tube diameter. As can be seen from Fig. 2(b), the tube thickness at the end of second half cycle in all channel angles reaches its initial value. This is an important feature of a SPD method.

Fig. 3 shows the plastic strain values through the thickness of processed tube at the end of second half cycle for all channel angles. It is clear that increase in the channel angle leads to decrease in strain. Up to channel angle 135°, the strain in the inner surface of the tube is a bit lower than that in the outer surface. This manner is changed in the channel angles higher than 135°. It may be because of formation of second corner gap in the channel angles higher than 135°. From this figure the strains of 4.4, 3.7, 3.05, 2.25, 1.55 and 1.05 are achieved for

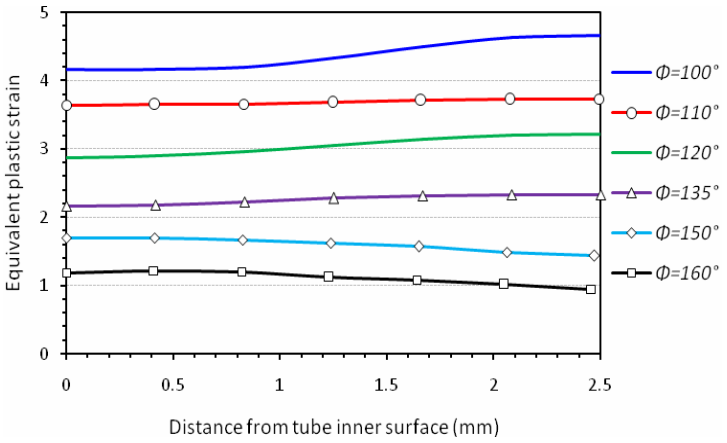

Fig. 3. Plastic strain values through the thickness of processed tube at the end of the second half cycle.

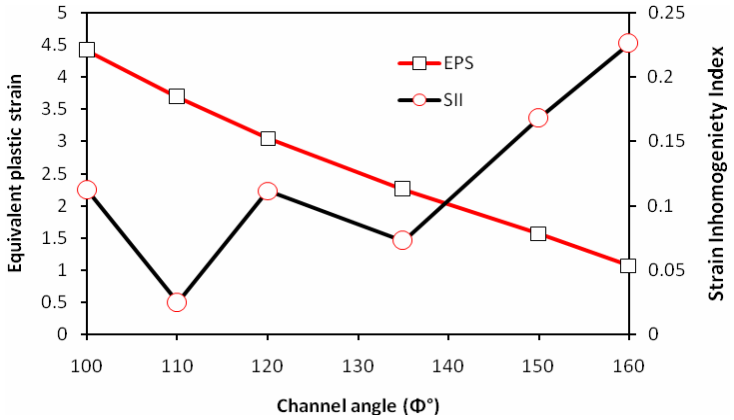

Fig. 4. Effect of channel angle on the mean strain value and strain inhomogeneity index.

channel angles of 100°, 110°, 120°, 130°, 140°, 150° and 160°, respectively. Internal microstructure homogeneity and consequently homogeneity in hardness measurements are greatly affected by homogeneity of induced plastic strains [18-20]. Therefore, Strain inhomogeneity index was defined to show the strain inhomogeneity as $SII = (\varepsilon_{Max} - \varepsilon_{Min}) / \varepsilon_{Ave.}$, where ε_{Max}, ε_{Min} and ε_{Ave} indicate maximum, minimum and average equivalent plastic strains along the processed tube thickness, respectively [20]. Fig. 4 shows the effects of channel angle on strain inhomogeneity index and means above the presented strain values. From this figure the trend of mean strain variation with channel angle is almost linear. Also, in strain inhomogeneity index curve, there is not a distinct trend in the channel angles up to 135°, but in higher angles it can be seen that increase in channel angle causes the increase of strain inhomogeneity index. In the other words, increase in the channel angle from 135° causes the decrease of strain homogeneity.

Fig. 5 (a) shows the effect of channel angle on load-displacement curve. Increase in the channel angle results the decrease in the required load. From the required instrument and energy consuming point of view, selecting higher channel angles is suitable. As it is shown, an interesting feature in the force history is that all curves are converged to a lower value. It may be attributed to the friction force, which is a normal force multiplied by a friction coefficient in the Coulomb friction model [14]. The tube during the TCAP process can be divided into two parts, i.e. the regions before and after the second shear zone. The hydrostatic pressure is higher in the regions before the last shear zone than that after the last shear zone. It means that the normal force in the region before the last shear zone is higher while in the region after the last shear zone it is going to have a lower value

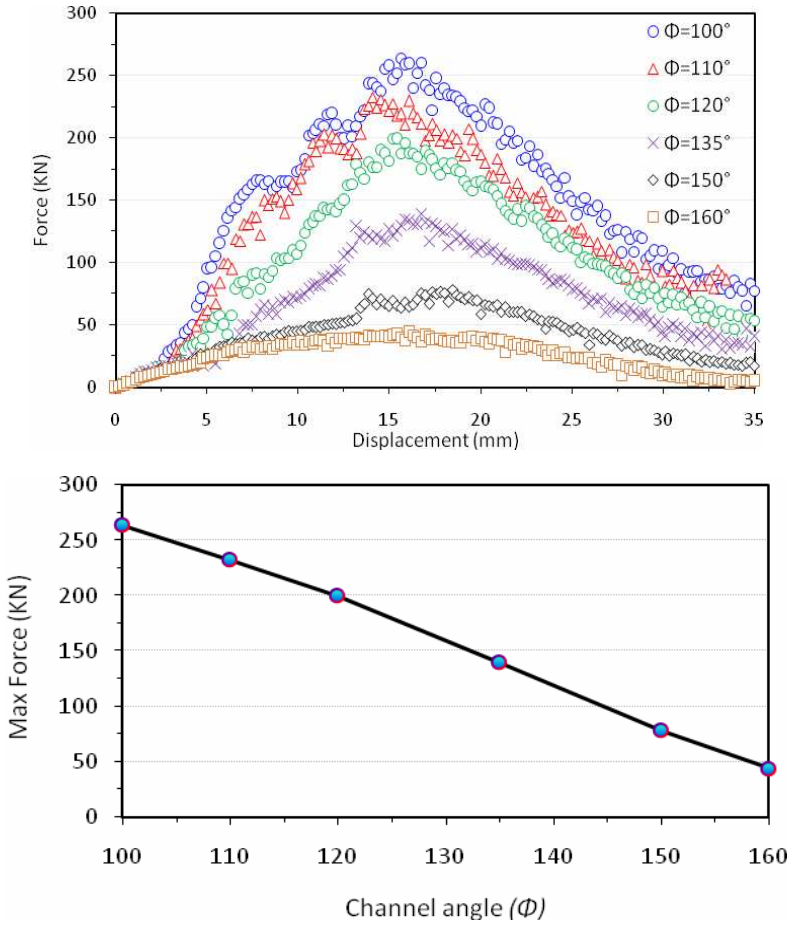

Fig. 5. (a) Force-displacement curves in different channel angles, (b) effect of the channel angle on the peak load.

[8]. When the first half cycle PTCAP proceeds, the tube length before the last shear zone is decreased and the tube length after the last shear zone is increased. Therefore, the total force is converged in all cases. The peak loads corresponding to different channel angles are shown in Fig. 5(b). The curve trend seems to be almost linear.

3. 2. Effects of curvature angle $\psi_1 = \psi_2$

Fig. 6 shows the effects of curvature angle $\psi_1 = \psi_2$ on pass plot of imposed strain through the PTCAP processed tube thickness. It can be seen that the change in the curvature angle has no effect on the imposed strain value in the inner surface of the processed tube, while an increase in the curvature angle causes a decrease in the strain level in the outer surface of the PTCAP processed tube. On the other hand, the strain homogeneity decreases when the curvature angle increases. Fig. 7 illustrates the effect of the curvature angle on the mean strain and strain inhomogeneity index through the thickness of PTCAP processed tube. An increase in the curvature angle up to 20° leads to a decrease in the mean strain value, while the change in the curvature angle values higher than 20° has almost no effect on it. Also, increase in the curvature angle up to 20° causes the increase in the strain inhomogeneity index but variation in the curvature angle higher than 20° has almost no effect on it. This means that better strain homogeneity is attainable in lower curvature angles.

Fig. 8 shows FE calculated load-displacement curves for different curvature angles in the PTCAP process. It is clearly seen from this figure that the variation in the curvature angle has almost no effect on the required load in the PTCAP process. So, from the point of view of required load and strain homogeneity it could be concluded that selecting the curvature angle

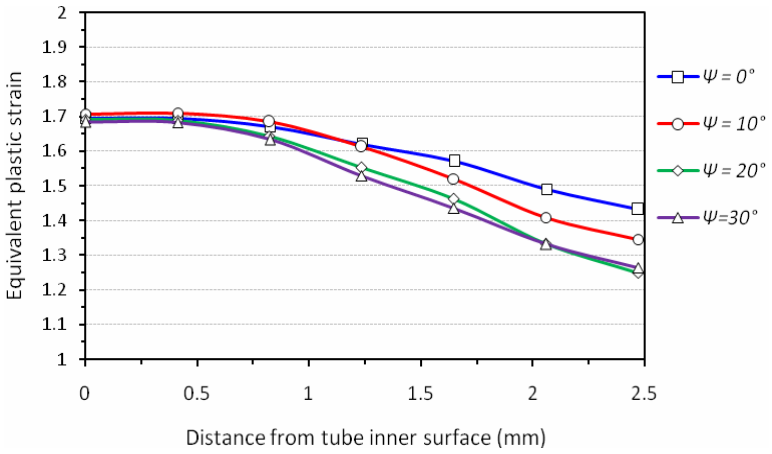

Fig. 6. Effect of curvature angle $\psi_1 = \psi_2$ on the pass plot of the imposed strain through tube thickness.

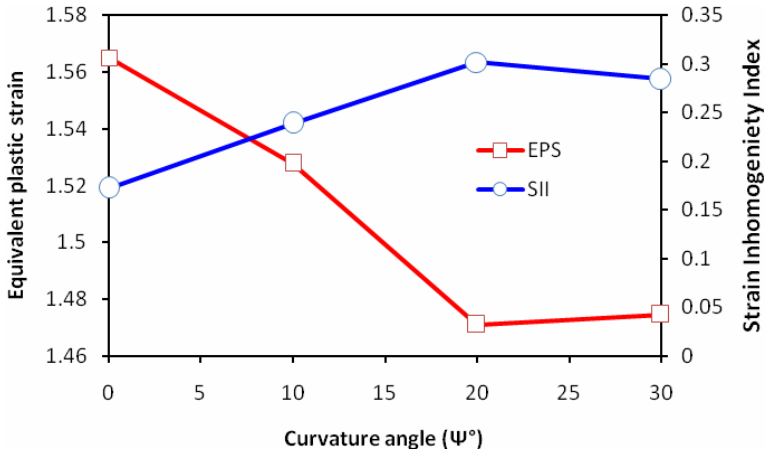

Fig. 7. Effect of the curvature angle on the mean strain and strain inhomogeneity index.

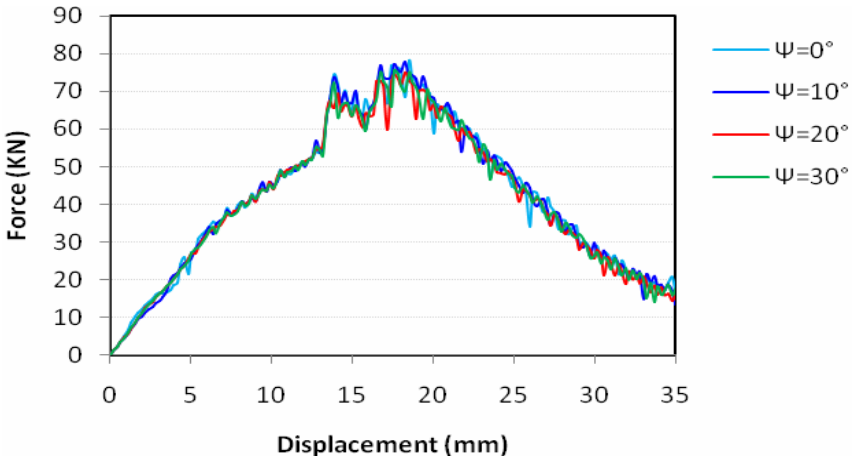

Fig. 8. FE calculated load-displacement curves in different curvature angles.

equal to zero is the best choice.

3. 3. Effects of the deformation ratio (K)

To investigate the effects of deformation ratio, the parameter $K = R_2 - R_1$ is considered. As it is shown in table 1, K values of 0.6 t_0, 0.8 t_0, 1 t_0, 1.2 t_0, and 1.4 t_0 were considered. Effect of the deformation ratio on pass plot of the

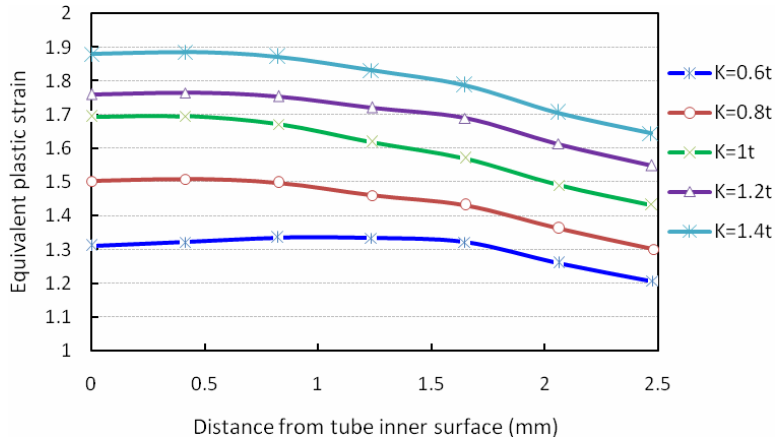

Fig. 9. Effect of deformation ratio (K) on the pass plot of the imposed strain through the PTCAP processed tube thickness.

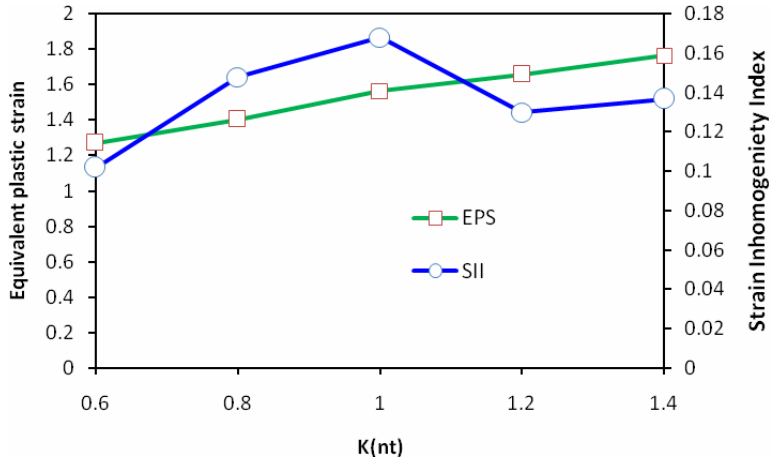

Fig. 10. Effect of K value on the mean strain and strain inhomogeneity index.

imposed strain through the PTCAP processed tube thickness is shown in Fig. 9. From this figure, increase in the deformation ratio K causes the increase in the imposed strain. It may be because the portion of equivalent plastic from normal strain due to variation of the tube diameter is changed when K value is varied. The trends of all curves are the same and in all cases the strain in the inner surface of the tube is higher than that in the outer surface. Fig. 10 shows the effect of K value on the mean equivalent strain and strain inhomogeneity index. The mean equivalent plastic strain increases almost linearly with the increase of K value. As it was mentioned before, whereas in PTCAP process the total equivalent strain contains both shear and normal components (resulted from tube diameter variations), linear increasing trend may be attributed to increase in the normal strain increasing. As can be seen in this figure, there exists no specific trend in strain inhomogeneity index curve. However, the best and worse strain homogeneity could be achieved in K equal to 0.6 and 1, respectively.

Fig. 11 (a) shows the effect of K value on FE calculated load-displacement curve in PTCAP process. Trends of all curves are similar while the positions of peak loads are different in various K values. the reason is that the distance between two shear zones differs for various K values. In higher K values the tube passes long trace between two consequent shear zones. Whereas the peak load is taking place in the last shear zone, the peak load position moves to the right as shown in Fig. 11(a). From Fig. 11(b) which shows the peak load versus K

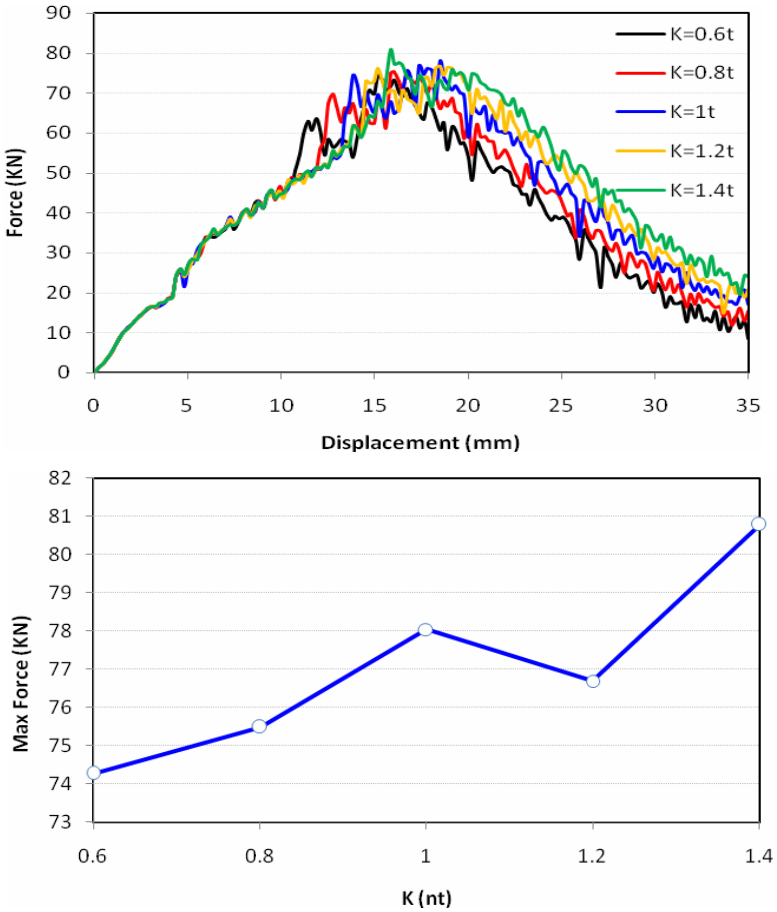

Fig. 11. Effect of K value on (a) load-displacement curve and (b) the peak required load.

value it could be realized that an increase in the K value leads to an increase in the peak load. So, from the point of view of better strain homogeneity and needing lower loads it could be concluded that lower K value (0.6) leads to best strain homogeneity and lowest process load.

4. Conclusions

The effects of PTCAP process parameters on plastic deformation behavior, imposed strain, strain homogeneity and required load were investigated using finite element method (FEM) and the results can be concluded as following:

- An increase in the channel angles leads to decrease in the imposed strain on the PTCAP processed tube.
- The curvature angle has no effect on the imposed strain in the inner surface of the processed tube.
- An increase in the curvature angle causes a decrease in the strain in the outer surface of the processed tube.
- Better strain homogeneity is achieved in lower curvature angles.
- Selection of the curvature angle equal to zero is the best choice from the point of view of requiring lower process load and better strain homogeneity.
- The best and worse strain homogeneity could be achieved in K equal to 0.6 and 1 respectively.
- From the point of view of better strain homogeneity and needing lower loads it could be concluded that lower K value ($0.6t_0$) leads to best strain homogeneity and lowest process load. So, selecting lower K value is the best choice.

Acknowledgements

The authors would like to acknowledge the financial support of Iran National Science

Foundation (INSF) for this research.

References

1. S.C. Yoon, P. Quang, S.I. Hong, H.S. Kim, "Journal of Materials Processing Technology", 187–188 (2007) 46-50.
2. T. Langdon, J Mater Sci, 42 (2007) 3388-3397.
3. K. Abrinia, M. Mirnia, The International Journal of Advanced Manufacturing Technology, 46 (2010) 411-421.
4. S.C. Yoon, Z. Horita, H.S. Kim, "Journal of Materials Processing Technology", 201 (2008) 32-36.
5. S. Lee, Y. Saito, N. Tsuji, H. Utsunomiya, T. Sakai, Scripta Materialia, 46 (2002) 281-285.
6. G. Faraji, H. Jafarzadeh, Materials and Manufacturing Processes, 27 (2012) 507-511.
7. A. Babaei, G. Faraji, M. Mashhadi, M. Hamdi, Materials Science and Engineering: A, (2012).
8. G. Faraji, M. Mashhadi, K. Abrinia, H. Kim, Applied Physics A: Materials Science & Processing, (2012) 1-9.
9. G. Faraji, M. M. Mashhadi, H. S. Kim, Materials Letters, (2011).
10. F. Ghader, M. M. Mosavi, K. H. Seop, Materials Transactions, 53 (2012) 8-12.
11. G. Faraji, M. Mashhadi, A. Dizadji, M. Hamdi, Journal of mechanical science and technology, 26 (2012) 3463-3468.
12. G. Faraji, A. Babaei, M.M. Mashhadi, K. Abrinia, Materials Letters, 77 (2012) 82-85.
13. G. Faraji, A. Bushroa, A. Babaei, M. Mashhadi, M. Hamdi, Materials Science and Engineering: A, (2012).
14. G. Faraji, M.M. Mashhadi, S.-H. Joo, H.S. Kim, Rev. Adv. Mater. Sci, 31 (2012) 12-18.
15. A. V. Nagasekhar, S. C. Yoon, Y. Tick-Hon, H.S. Kim, Computational Materials Science, 46 (2009) 347-351.
16. F. Djavanroodi, M. Ebrahimi, Materials Science and Engineering: A, 527 (2010) 1230-1235.
17. H. S. Kim, Materials Science and Engineering: A, 328 (2002) 317-323.
18. C. Xu, M. Furukawa, Z. Horita, T.G. Langdon, Acta Materialia, 51 (2003) 6139-6149.
19. C. Xu, Z. Horita, T.G. Langdon, Acta Materialia, 55 (2007) 203-212.
20. C. Xu, K. Xia, T.G. Langdon, Acta Materialia, 55 (2007) 2351-2360.